ompg-C_3N_4/SO_3H: an efficient and recyclable organocatalyst for the facile synthesis of 2,3-dihydroquinazolin-4(1H)-ones

Hossein Ghafuri[1] · Nahal Goodarzi[1] · Afsaneh Rashidizadeh[1] · Mohammad Ali Douzandegi Fard[1]

Abstract

In the present work, sulfonated highly ordered mesoporous graphitic carbon nitride (ompg-C_3N_4/SO_3H) was synthesized successfully and employed as an efficient and reusable heterogeneous solid acid catalyst for the rapid and one-pot synthesis of 2,3-dihydroquinazolin-4(1H)-ones via the condensation of anthranilamide with aldehydes or ketones in good to excellent yields. The organocatalyst was characterized by Fourier transform infrared spectroscopy, X-ray diffraction, field emission scanning electron microscopy, energy-dispersive X-ray spectrometer, Brunauer–Emmett–Teller surface area, and thermal gravimetric and differential thermal analysis. The substantial advantages of this procedure involve short reaction times, high catalytic activity, easy workup, high purity of the products, and easy recovery and reusability of the catalyst.

Keywords Sulfonated highly ordered mesoporous graphitic carbon nitride (ompg-C_3N_4/SO_3H) · 2,3-dihydroquinazolin-4(1H)-ones · Organocatalyst · Green procedure

Introduction

Nowadays, solid acid catalysts are receiving considerable attention in organic synthesis and transformation because of their various benefits including: chemical stability, high activity, non-toxicity, non-corrosiveness, high selectivity, easy separation and reusability without losing activity, simplicity of operation and carrying out reactions

✉ Hossein Ghafuri
ghafuri@iust.ac.ir

1 Catalysts and Organic Synthesis Research Laboratory, Department of Chemistry, Iran University of Science and Technology, Tehran 16846-13114, Iran

in an economic and green route [1]. There are several factors that influence the properties and performance of the solid acid catalysts such as: type of acidity (Bronsted or Lewis), strength of the acidic sites, availability of these sites, and morphology of the support in terms of surface area, porosity and stability (thermal and chemical). Hence, applying a suitable support can improve the function of these catalysts [2].

Among the organic polymeric compounds, graphite carbon nitride (g-C_3N_4) has attracted tremendous attention in various fields as photocatalysis, solar cells, sensing, solar fuel production, and catalysis due to its special structure and fascinating electronic properties [3–7]. g-C_3N_4 with an environmentally friendly nature and extreme thermal and chemical stability can be easily synthesized at a low price with abundant nitrogen-rich carbon materials such as cyanamide, dicyanamide, melamine, urea, and thiourea through thermal condensation [8]. Metal-free g-C_3N_4 as a π-conjugated polymer with an electron-rich surface is a promising support material due to the incorporation of nitrogen atoms into a carbon architecture. The presence of amino functional groups with abundant basic sites in the g-C_3N_4 leads to loading high amounts of active chemical sites on the g-C_3N_4. Basically, strong Van der Waals interactions between the layers in the two-dimensional g-C_3N_4 framework convert this material to the most chemically stable allotrope against various organic solvents, and several acids and bases. Also, the existence of aromatic C–N heterocycles, leads to thermal stability up to 600 °C. Given the mentioned advantages and with the aim to broaden the potential of g-C_3N_4 with reasonable physical and chemical properties, non-toxicity, high specific surface area, easy recyclability, abundant anchor sites for active species and environmentally friendly nature, g-C_3N_4 is appropriate for the design of high-performance catalysts or catalyst support. [9].

Creation of porosity in the structure of g-C_3N_4 and producing a hexagonally ordered mesoporous structure improves its properties and applications as a catalyst support. As compared to bulk g-C_3N_4, ordered mesoporous g-C_3N_4 (ompg-C_3N_4) exhibits more excellent properties such as high specific surface area, more surface active sites, large pore volume, and strong adsorption capacity [10, 11].

Recently, the template-directed synthesis methods, including the use of mesoporous silica materials (SBA-15, KIT-6, and FDU-12) have been widely applied to prepare mesoporous g-C_3N_4 which can control the morphology and the pore structure of the target mesoporous g-C_3N_4 [11]. SBA-15 is a common material for hard templating protocols due to its advantages such as simple preparation using inexpensive precursor (tetraethyl orthosilicate), high thermal and hydrothermal stability, and tunable pore size [12].

In the course of our investigations on developing novel heterogeneous catalysts for the synthesis of organic compounds [13–16], we have recently reported the preparation of sulfonated highly ordered mesoporous graphitic carbon nitride (ompg-C_3N_4/SO_3H) and its application as a super-active solid acid catalyst for Biginelli reaction [17].

2,3-Dihydroquinazolin-4(1*H*)-one derivatives are a significant class of bicyclic heterocycles and useful intermediates in organic synthesis with a broad range of medical, biological and pharmaceutical activities such as antioxidant, anticancer [18], antibacterial [19], anti-inflammatory [20], and antibiotic [21] activity. Conventionally, 2,3-dihydroquinazolin-4(1*H*)-ones are synthesized using the condensation reaction of 2-aminobenzamide with aldehydes or ketones in the presence of various catalysts. In view of the importance of the 2,3-dihydroquinazolin-4(1*H*)-ones, a

number of catalysts have been reported for the preparation of 2,3-dihydroquinazolin-4(1*H*)-one derivatives in literature, which include tetrabutylammonium bromide [22], succinimide-*N*-sulfonic acid [23], [Emim] HSO₄ [24], Sc(OTF)₃ [25], and L-proline nitrate [26]. However, some of the mentioned procedures suffer from one or several limitations such as longer reaction times, harsh reaction conditions, low product yields, the use of volatile organic solvents, and hard work-up procedure. Therefore, the development of environmentally friendly synthetic methodologies using novel heterogeneous catalysts for the synthesis of these compounds is still in great demand.

Herein we investigated the efficiency of ompg-C₃N₄/SO₃H as a green and recoverable heterogeneous catalyst for the synthesis of 2,3-dihydroquinazolin-4(1*H*)-ones in excellent yields (Scheme 1). The novel solid acid (ompg-C₃N₄/SO₃H) is expected to have a broader potential in chemical processes as a heterogeneous catalyst due to high activity, strong acidity strength, thermal stability, and reusability.

Experimental

Chemicals and instruments

All utilized chemicals and solvents such as P123, TEOS, ammonium hydrogen difluoride, cyanamide, chlorosulfonic acid, aldehydes and ketones, 2-aminobenzamide, solvents and other materials were purchased from Merck and Flucka chemical companies and used without any purification. The reaction progress was followed by thin-layer chromatography (TLC) using aluminum plates coated with silica gel F254. Melting points were measured using an Electrothermal 9100. The FT-IR spectra were measured with a Shimadzu 800 IR 100 FT-IR spectrometer using a KBr pellet. The morphology of the catalyst was discerned via field-emission scanning electron microscopy (FESEM) using a MRIA3 TESCAN-XMU model and transmission electron microscopy (TEM) on a Zeiss-EM10C-100 kV. The powder X-ray diffraction (XRD) patterns of the samples were obtained on a PANalytical X-PERT-PRO MPD diffractometer equipped with a Cu Kα radiation source ($\lambda = 1.5406$ Å) in the $2\theta = 0.5°$ to 10° and $2\theta = 10°$ to 80° with a 2θ step size of 0.02°. Energy-dispersive X-ray (EDX) spectra were determined using a Numerix DXP-X10P. The C, H, N, and S elemental analyses were recorded using a Thermo Finnigan Flash EA 1112 element analyzer. Thermogravimetric analysis (TGA) and differential thermal analysis (DTG) were conducted under air using a STA504 analyzer with a 10 °C/min ramp in the range of 20–800 °C. Nitrogen adsorption and desorption measurements were carried out using Micromeritics ASAP 2020 device with nitrogen as the
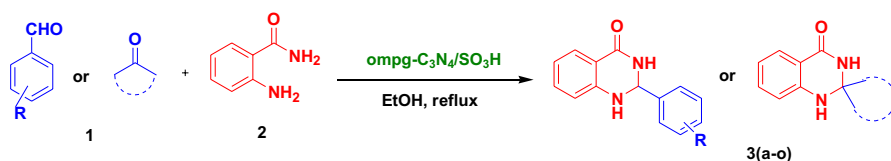
Scheme 1 Synthesis of 2,3-dihydroquinazolin-4(1*H*)-one derivatives catalyzed by ompg-C₃N₄/SO₃H

analysis gas at −196 °C. BET analysis was conducted to investigate the specific surface areas and the pore size distributions were obtained on the adsorption branches of the isotherms using a Brunauer–Joyner–Halenda (BJH) model. The nuclear magnetic resonance (NMR) spectra, in order to identify products, were obtained on a Bruker DRX-500 Avance spectrometer (500 MHz for ^{1}H NMR) using DMSO-d$_6$ as a solvent and tetramethylsilane (TMS) as an internal standard.

Synthesis of the mesoporous silica (SBA-15)

Synthesis of SBA-15 (as a hard template for the preparation of ompg-C$_3$N$_4$/SO$_3$H) was carried out according to the procedure reported previously in the literature [27]. Initially, 3.5 g of Pluronic P123 was dissolved in 120.0 mL of 1.6 M HCl and stirred for 24 h at 38 °C. Afterward, 7.5 g of tetraethylorthosilicate (TEOS) was added dropwise into the above mixture during stirring. After 24 h, the resulting milky liquid was transferred into the Teflon-lined autoclave and heated at 150 °C for 24 h. The obtained white precipitate was filtered and frequently washed with de-ionized water then dried at ambient temperature and calcined at 550 °C with a heating rate of 2.3 °C min^{-1} for 5 h.

Preparation of the ordered mesoporous graphite carbon nitride (ompg-C$_3$N$_4$)

At the first step, 1.0 g of SBA-15 (as a hard template) and 3.5 g of cyanamide were added to 8.0 mL of de-ionized water and sonicated for 2 h. The mixture was then stirred at ambient temperature for 6 h. The obtained white precipitate was filtrated and dried at 60 °C. Then it was calcined at 550 °C in a furnace under nitrogen atmosphere for 5 h. Next, in order to remove the silica template, the obtained yellow precipitate was added to 40.0 mL of NH$_4$·HF$_2$ (4.0 M) aqueous solution while stirring at ambient temperature for 24 h. Eventually, the solid product was filtered and washed with de-ionized water and ethanol for several times, and dried at 60 °C.

Synthesis of mesoporous graphite carbon nitride nanocomposite functionalized by sulfonic acid (ompg-C$_3$N$_4$/SO$_3$H)

1.0 g of ompg-C$_3$N$_4$ was dispersed in 5.0 mL of dry CH$_2$Cl$_2$. After that, in order to conduct HCl gas over the solution, the mixture was transferred into a suction flask that was equipped with a gas inlet tube. Afterward, ClSO$_3$H (2.0 mL) was added dropwise into the mixture vessel for 30 min and then the mixture was stirred for 2 h. Finally, the solvent was evaporated under reduced pressure, and the obtained product was washed with de-ionized water and methanol for several times and dried at 60 °C.

General procedure for the preparation of 2,3-dihydroquinazolin-4(1*H*)-ones

A mixture of 2-aminobenzamide (1.0 mmol), aldehyde (or ketone) (1.0 mmol), and ompg-C$_3$N$_4$/SO$_3$H (20.0 mg) in 96% EtOH (3.0 mL) was stirred under reflux condition for an appropriate time (Table 3). Progression of the reaction was followed by TLC (hexane/EtOAc 2:1). After completion of the reaction, the catalyst was separated

by filtration and washed with ethanol for reuse in subsequent reactions. After evaporation of the solvent, the residue was purified by recrystallization from ethanol.

Back-titration in aqueous solution of catalyst (ompg-C$_3$N$_4$/SO$_3$H)

Back-titration procedure as a well-known method for determining the concentration of [H$^+$] ion released by the ompg-C$_3$N$_4$/SO$_3$H was used. A mixture of 0.5 g ompg-C$_3$N$_4$/SO$_3$H, 0.5 g NaCl, 10.0 mL of 0.1 M NaOH aqueous solution, and 35.0 mL of distilled water was added into an Erlenmeyer flask and stirred at room temperature for 24 h. Afterward, three drops of phenolphthalein, as an indicator, were added to the above solution then titrated with 0.1 M HCl aqueous solution until the color of the solution turns from pink to colorless. The pH value of the ompg-C$_3$N$_4$/SO$_3$H was calculated (pH = 1.55).

Selected spectral data

2,3-dihydro-2-phenylquinazolin-4(1H)-one (3a)

White solid; mp 229–232 °C; FTIR (KBr, cm^{-1}): 3299, 3184, 1506, 3062, 1658, 1612, 1440, 1386, 746; ^{1}HNMR (500 MHz, DMSO-d$_6$) δ 8.30 (s,1H, –NH), 7.20–7.63 (m, 7H, Ar–H), 7.15 (s, 1H, CH), 6.65–6.77 (m, 2H, Ar–H), 5.75 (s, 1H, –NH).

2,3-dihydro-2-(2-chlorophenyl)quinazolin-4(1H)-one (*3h*)

White solid; mp 207–209 °C; FTIR (KBr, cm^{-1}): 3363, 3197, 3060, 2912, 1650, 1608, 1496, 1475, 1458, 1035, 746; ^{1}HNMR (500 MHz, DMSO-d$_6$) δ 8.19 (s,1H, –NH), 7.65–7.64 (d, 2H, Ar–H, $J = 6.4$ Hz), 7.23–7.50 (m, 4H, Ar–H), 7.00 (s, 1H, –CH), 6.68–6.77 (m, 2H, Ar–H), 6.13 (s, 1H, –NH).

1H-Spiro(cyclohexane-1,2-quinazolin)-4(3H)-one (*3m*)

White solid; mp 223–227 °C; FTIR (KBr, cm^{-1}): 3361, 3179, 2927, 2858,1645, 1490, 1390, 1137, 756; ^{1}H NMR (500 MHz, DMSO-d$_6$) δ 7.90 (s, 1H, –NH), 7.56 (d, $J = 7.6$ Hz, 1H, –CH), 7.21 (t, $J = 7.6$ Hz, 1H, –CH), 6.80 (d, $J = 8.1$ Hz, 1H, –CH), 6.62 (d, $J = 7.4$ Hz, 1H, –CH), 6.60 (s, 1H, –NH), 1.73 (s, 2H, –CH), 1.66–1.48 (m, 6H, –CH$_2$), 1.42 (s, 1H, –CH), 1.31–1.19 (m, 1H, –CH).

1H-Spiro(cyclopentane-1,2-quinazolin)-4(3H)-one (*3n*)

White solid; mp 256–258 °C; FTIR (KBr, cm^{-1}): 3290, 3163, 2941, 2848, 1637, 1612, 1429, 1380, 754; ^{1}H NMR (500 MHz, DMSO-d$_6$) δ 8.07 (s, 1H, –NH), 7.56

(d, $J = 5.7$ Hz, 1H, –CH), 7.20 (t, $J = 7.2$ Hz, 1H, –CH), 6.73 (s, 1H, –NH), 6.68 (d, $J = 8$ Hz, 1H, –CH), 6.62 (t, $J = 7.5$ Hz, 1H, –CH), 1.78 (s, 4H, –CH), 1.65 (s, 4H, –CH).

Results and discussion

Catalyst characterizations

The highly ordered mesoporous graphitic carbon nitride (ompg-C_3N_4) was prepared via a facile template-assisted method using SBA-15 as a mesoporous silica template and functionalized with sulfonic acid (ompg-C_3N_4/SO_3H). The structure of ompg-C_3N_4 and ompg-C_3N_4/SO_3H were proved by some analyses. The small-angle region of the XRD patterns was analyzed to ascertain the hexagonal mesoporous structure of ompg-C_3N_4 (Fig. 1a). A peak appeared at $2\theta = 0.9°$, and the other one at $2\theta = 1.6°$ proved the mesostructural order of the hexagonal framework for ompg-C_3N_4 [28–30]. The wide-angle regions of XRD patterns of ompg-C_3N_4 and ompg-C_3N_4/SO_3H demonstrate two obvious peaks at about $2\theta = 27.4°$ and $13.6°$ (Fig. 1b). The peak appearing at $2\theta = 27.4°$ with higher
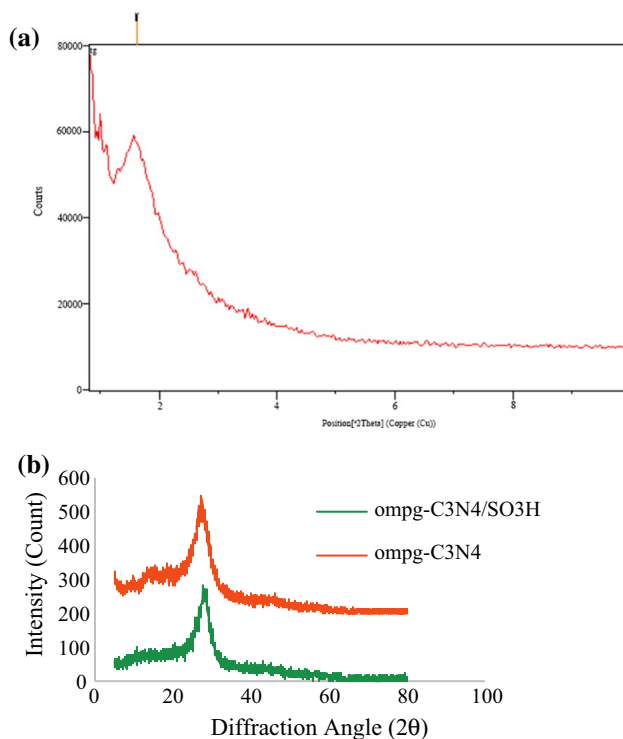

Fig. 1 **a** Small-angle XRD pattern of ompg-C_3N_4 and **b** wide-angle XRD patterns of ompg-C_3N_4 and ompg-C_3N_4/SO_3H

intensity indexed as the (002) planes belongs to the interlayer stacking existent in the conjugated aromatic ring of the crystalline graphitic carbon nitride structure. Another peak with lower intensity at $2\theta = 13.6°$ indexed as the (100) planes corresponds to the in-plane structural repeating unit close to tris-s-triazine. The intensity of both reflections decreases during the functionalization.

The FT-IR spectra of ompg-C$_3$N$_4$ and ompg-C$_3$N$_4$/SO$_3$H are shown in Fig. 2. The broad peaks at about 3000–3500 cm^{-1} are attributed to –NH and –NH$_2$ stretching vibrations that confirm the existence of amino groups and show hydrogen bonding interactions between the functional groups in the composition structure. The peaks related to stretching vibrations of heterocyclic s-triazine rings were seen in the region of 900–1700 cm^{-1}. The characteristic peaks at 1307 cm^{-1} and 1602 cm^{-1} can be ascribed to the C–N and C=N stretching vibration, respectively. The observed peak at 806 cm^{-1} is associated to tri-s-triazine units. The spectrum of ompg-C$_3$N$_4$/SO$_3$H also shows the vibration bands at 1049 cm^{-1} (S=O symmetric stretching), 1149 cm^{-1} (S=O asymmetric stretching), and 1413 cm^{-1} (asymmetric SO$_2$ stretching in SO$_3$H) that are related to SO$_3$H groups. Of note, these peaks might be overlapped with the typical stretching bands of CN heterocycles.

The morphologies of ompg-C$_3$N$_4$ and ompg-C$_3$N$_4$/SO$_3$H were investigated by field-emission scanning electron microscopy (FESEM) and transmission electron microscopy (TEM) images. The images obtained of ompg-C$_3$N$_4$ and ompg-C$_3$N$_4$/SO$_3$H confirm the uniform structures with typical rod-like morphology. The images of ompg-C$_3$N$_4$/SO$_3$H obviously show that the ompg-C$_3$N$_4$ is functionalized with SO$_3$H groups successfully (Fig. 3).

EDX spectroscopy analysis was utilized for characterization of elements in the structure of ompg-C$_3$N$_4$/SO$_3$H (Fig. 4). This analysis confirms the existence of C, N, S, and O elements in the structure of ompg-C$_3$N$_4$/SO$_3$H, and proves that the surface of the ompg-C$_3$N$_4$ is functionalized with SO$_3$H groups. The absence of an Si peak demonstrates that the silica template was removed entirely from ompg-C$_3$N$_4$ by washing with NH$_4$HF$_2$. Also, elemental analysis was applied for the determination precise amounts of C, H, N, and S in the structure of ompg-C$_3$N$_4$/SO$_3$H. According to this analysis, the existence of 27.83%, 2.91%, 47.06%,
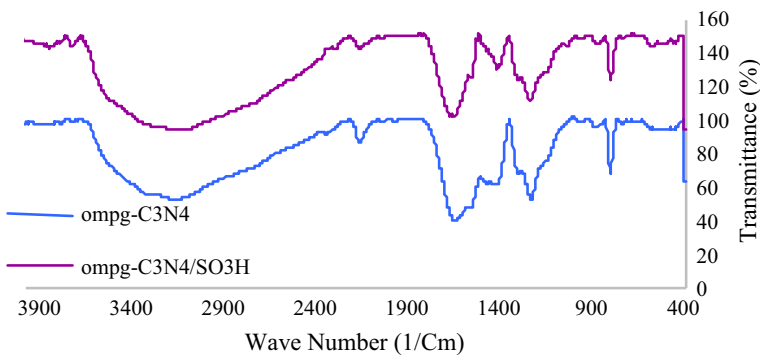

Fig. 2 The FT-IR spectra of the ompg-C$_3$N$_4$ and ompg-C$_3$N$_4$/SO$_3$H
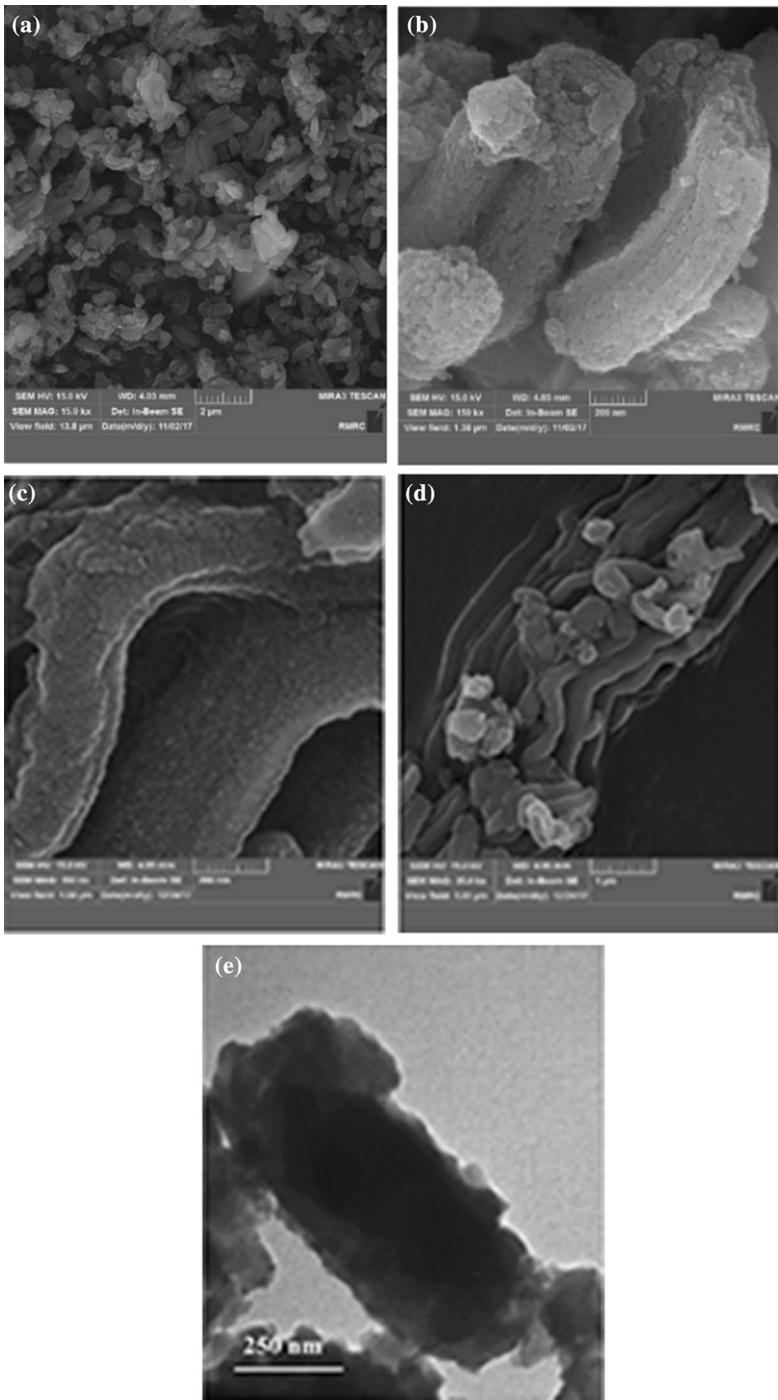
Fig. 3 FESEM photographs of ompg-C_3N_4 (**a**, **b**), ompg-C_3N_4/SO_3H (**c**, **d**), and TEM image of ompg-C_3N_4/SO_3H (**e**)
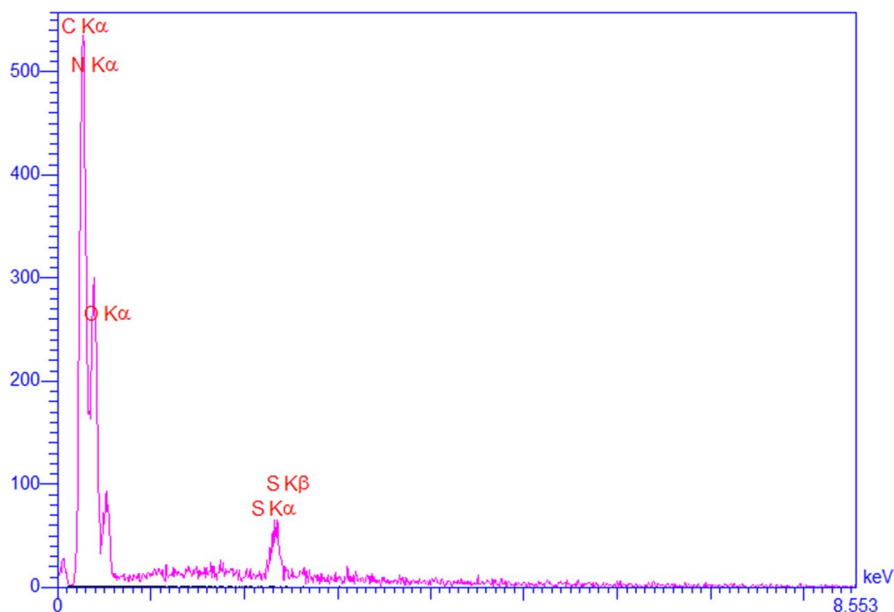
Fig. 4 EDX analysis of the ompg-C$_3$N$_4$/SO$_3$H

Table 1 Porous characteristics of the ompg-C$_3$N$_4$ and ompg-C$_3$N$_4$/SO$_3$H

Sample	S_{BET} (m^2 g^{-1})	Pore volume^a (cm^3 g^{-1})	Pore size (nm)
ompg-C$_3$N$_4$	73.8	0.128	5.4
ompg-C$_3$N$_4$/SO$_3$H	14.2	0.075	18.7

^{a}Determined at $p/p^0 = 0.97$, where p is the equilibrium pressure and p^0 is the saturation pressure of nitrogen at -196 °C

and 2.72% of C, H, N, and S elements, respectively, in the ompg-C$_3$N$_4$/SO$_3$H was proved.

BET analysis was performed to estimate the specific surface area, pore volume, and the pore size of the ompg-C$_3$N$_4$ and ompg-C$_3$N$_4$/SO$_3$H (Table 1). After immobilization of sulfonic groups on the ompg-C$_3$N$_4$, the total pore volume and the BET surface area decreased from 0.128 cm^3 g^{-1} and 73.8 m^2 g^{-1} for ompg-C$_3$N$_4$ to 0.075 cm^3 g^{-1} and 14.2 m^2 g^{-1} for ompg-C$_3$N$_4$/SO$_3$H, which confirms the immobilization of sulfonic groups clearly (Fig S1).

The thermal stability of ompg-C$_3$N$_4$ and ompg-C$_3$N$_4$/SO$_3$H was examined using TGA and differential thermal analysis (DTA) under nitrogen atmosphere at the range of 50 °C to 800 °C, at a heating rate of 10 °C/min (Fig. 5). The first weight loss (approximately 6%) appeared at 100–200 °C, resulting from the removal of adsorbed water and other volatile impurities from the catalyst. Another weight loss occurred at about 400–500 °C, corresponding to the elimination of a sulfonic group. Eventually, sharp weight loss appeared at above 600 °C that belongs to the thermal
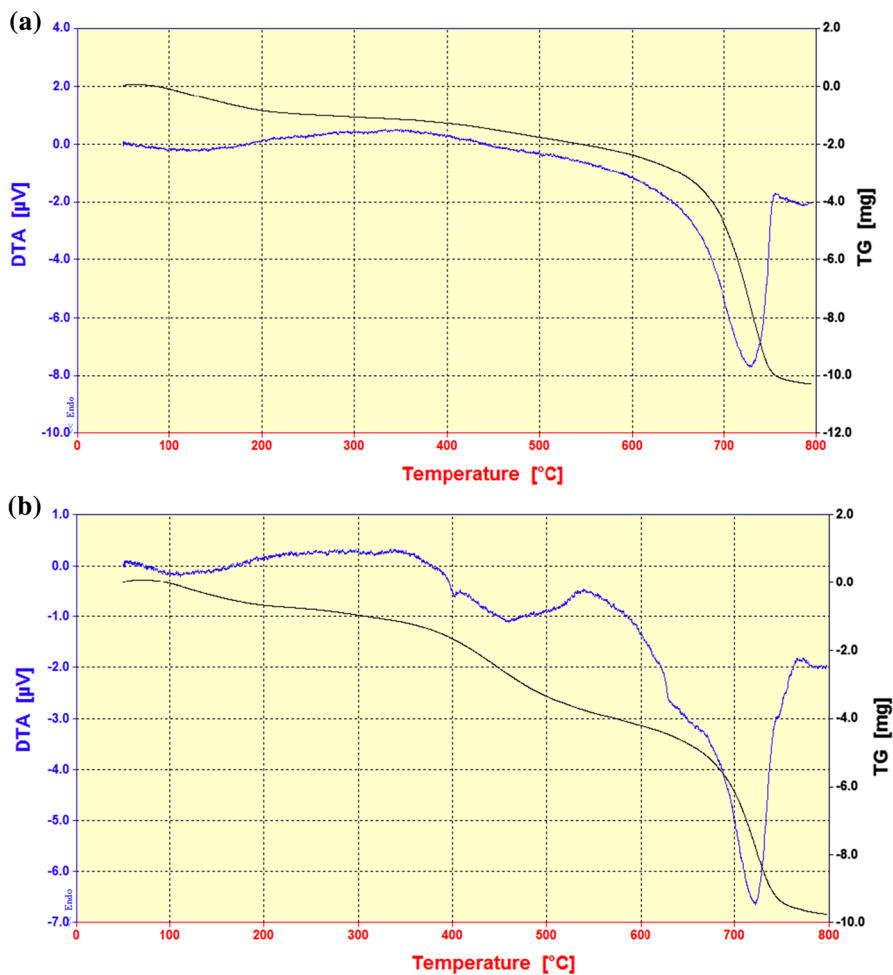
Fig. 5 TGA/DTA curves of the **a** ompg-C$_3$N$_4$ and **b** ompg-C$_3$N$_4$/SO$_3$H

decomposition of g-C$_3$N$_4$ which confirms the high thermal stability of ompg-C$_3$N$_4$/SO$_3$H.

The efficiency and catalytic performance of the ompg-C$_3$N$_4$/SO$_3$H was evaluated for the one-pot synthesis of 2,3-dihydroquinazolin-4(1H)-one derivatives. This process was carried out via the condensation reaction between carbonyl compounds (aldehydes or ketones) and 2-aminobenzamide as precursors. Our initial efforts concentrated on designing an eco-friendly method with the best reaction conditions in terms of time, yield, and the amount of catalyst. Thus, the condensation reaction between benzaldehyde (1.0 mmol) and 2-aminobenzamide (1.0 mmol) was chosen as a model reaction, and the effect of several solvents, different amount of catalyst, and varying temperature on the reaction was investigated (Table 2).

Table 2 Optimization of the reaction conditions for the condensation of benzaldehyde and 2-aminobenzamid as the model reaction for the one-pot synthesis of 2,3-dihydroquinazolin-4(1H)-ones

Entry	Solvent	Amount of catalyst (mg)	Temp. (°C)	Time (min)	Yield[a] (%)
1	MeOH	–	Reflux	120	–
2	EtOH	–	Reflux	120	–
3	H$_2$O	–	Reflux	120	–
4	–	–	120	120	–
5	MeOH	10	RT	5	89
6	EtOH	10	RT	5	89
7	H$_2$O	10	RT	5	83
8	Ball milling	10	RT	5	86
9	–	10	120	5	87
10	H$_2$O	10	Reflux	10	84
11	EtOH	10	60	5	91
12	EtOH	10	Reflux	3	94
13	EtOH	5	Reflux	3	89
14	EtOH	15	Reflux	3	94
15	EtOH	20	Reflux	3	98
16	EtOH	30	Reflux	3	98
17	EtOH	(ompg-C$_3$N$_4$, 20 mg)	Reflux	3	Trace

RT room temperature. Reaction conditions: benzaldehyde (1.0 mmol), 2-aminobenzamide (1.0 mmol), catalyst: ompg-C$_3$N$_4$/SO$_3$H, solvent (3.0 mL)
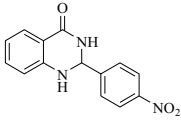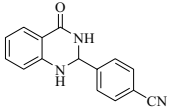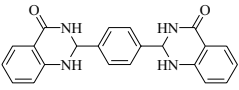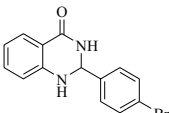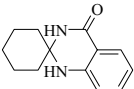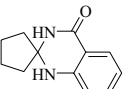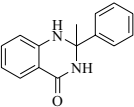
[a]Isolated yield

First, we applied a variety of solvents such as MeOH, EtOH, H$_2$O, and also solvent-free condition (Table 2, entries 1–5). As shown in Table 2, no target products were detected when the reaction was performed in the absence of any catalysts (Table 2, entries 1–4), whereas using ompg-C$_3$N$_4$/SO$_3$H as a catalyst gave satisfactory results. Among these solvents and solvent-free conditions, ethanol was found to be most efficient for producing satisfactory results (Table 2, entry 6). In order to assess the effect of temperature, the model reaction was conducted at different temperatures like room temperature, 60 °C, and reflux temperature (Table 2, entries 6, 11, 12).

It was observed that increasing the reaction temperature to 80 °C (reflux temperature) led to the improvement of the yield of the desired product. To assess the catalytic activity of sulfonated ordered mesoporous graphitic carbon nitride (ompg-C$_3$N$_4$/SO$_3$H), ompg-C$_3$N$_4$ was examined as a catalyst in the model reaction (Table 2, entry 17). As shown, the catalytic activity of ompg-C$_3$N$_4$/SO$_3$H is greater than ompg-C$_3$N$_4$ (catalyst support) for this reaction. Finally, the optimal amount of the catalyst was explored by varying the amount of the catalyst in the model reaction (Table 2, entries 12–16). The results showed that the excellent yield (98%) of the target product results when 20 mg of catalyst was used in the reaction (Table 2, entry 15), and further increasing the amount of catalyst has no significant effect on the reaction time and yield in the same reaction conditions (Table 2, entry 16).

Table 3 The ompg-C$_3$N$_4$/SO$_3$H-catalyzed reaction in the presence of various aldehydes or ketones for synthesis of 2,3-dihydroquinazolin-4(1H)-one derivatives

Entry	Carbonyl compound	Product	Time (min)	Yield[a] (%)	M.p (observed) (°C) [Ref.]
1	PhCHO	(3a)	3	98	229–232 [31]
2	4-(Cl)C$_6$H$_4$CHO	(3b)	15	91	203–206 [23]
3	4-(Me)C$_6$H$_4$CHO	(3c)	5	96	232–234 [32]
4	4-(OH) C$_6$H$_4$CHO	(3d)	15	78	213–215 [33]
5	4-(OMe) C$_6$H$_4$CHO	(3e)	15	73	178–182 [34]
6	3-(NO$_2$) C$_6$H$_4$CHO	(3f)	10	93	199–202 [35]
7	4-(F) C$_6$H$_4$CHO	(3g)	3	95	193–197 [36]
8	2-(Cl) C$_6$H$_4$CHO	(3h)	8	92	207–209 [37]

Table 3 (continued)

Entry	Carbonyl compound	Product	Time (min)	Yield[a] (%)	M.p (observed) (°C) [Ref.]
9	4-(NO$_2$) C$_6$H$_4$CHO	(3i)	12	91	200−202 [38]
10	4-(CN) C$_6$H$_4$CHO	(3j)	5	91	349−351 [39]
11	Terephthaldehyde	(3k)	7	87	242−246 [40]
12	4-(Br) C$_6$H$_4$CHO	(3l)	3	96	196−198 [23]
13	Cyclohexanone	(3m)	3	96	223−227 [41]
14	Cyclopentanone	(3n)	7	94	256−258 [42]
15	Acetophenone	(3o)	3	98	221−224 [43]

Reaction conditions: aldehydes or Ketones (1.0 mmol), 2-aminobenzamide (1.0 mmol), catalyst (20.0 mg), EtOH (3.0 mL), under reflux condition

[a]Isolated yield
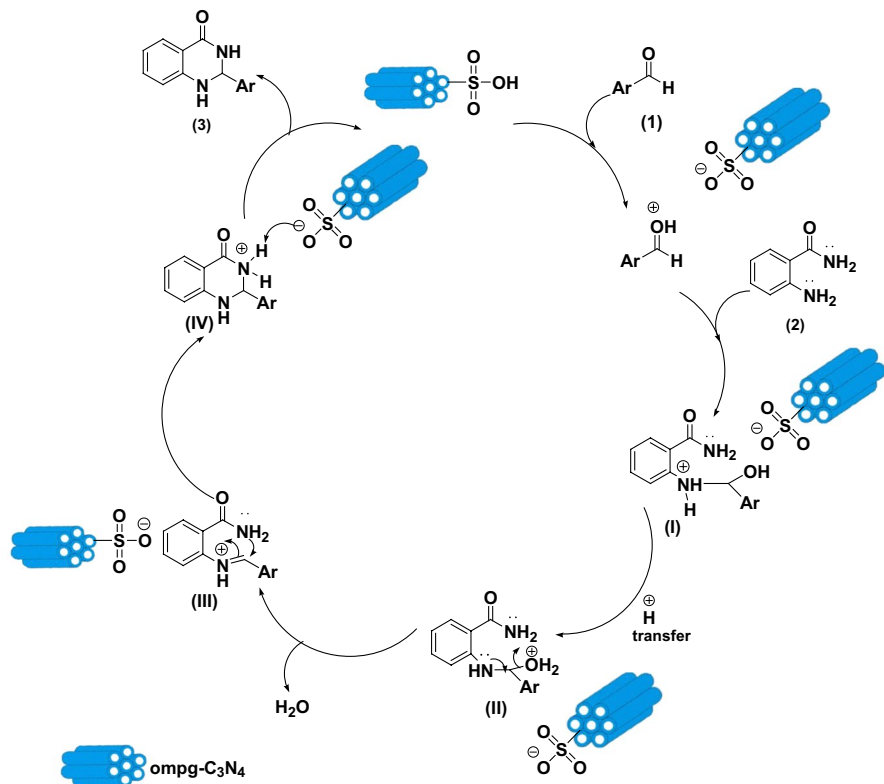
Scheme 2 Suggested mechanism for the synthesis of 2,3-dihydroquinazolin-4(1*H*)-one derivatives catalyzed by ompg-C$_3$N$_4$/SO$_3$H

With the optimized conditions, in order to evaluate the scope and generality of this protocol, the reaction was carried out with various substituted aromatic aldehydes (Table 3, entries 1–13), as well as ketones such as cyclohexanone and cyclopentanone (Table 3, entries 14–15). It was observed that the protocol was effective with aromatic aldehydes having either electron-donating (−OMe, −OH, Me) or electron-withdrawing (−F, −Cl, −Br, −CN, −NO$_2$) groups and also ketones to produce the desired products in high yields.

The possible mechanism for the formation of 2,3-dihydroquinazolin-4(1*H*)-ones in the presence of ompg-C$_3$N$_4$/SO$_3$H as a solid acid catalyst is shown in Scheme 2. At the first step of this reaction, ompg-C$_3$N$_4$/SO$_3$H as a Bronsted acid activates the carbonyl functional group of aldehyde or ketone (**1**) through protonation. Thereafter, the activated carbonyl group with high electrophilicity is attacked by the amino group in 2-aminobenzamide (**2**) during nucleophilic addition to give an intermediate (**I**). Subsequently, proton transfer forms intermediate (**II**). Afterward, an iminium ion intermediate (**III**) is formed through dehydration
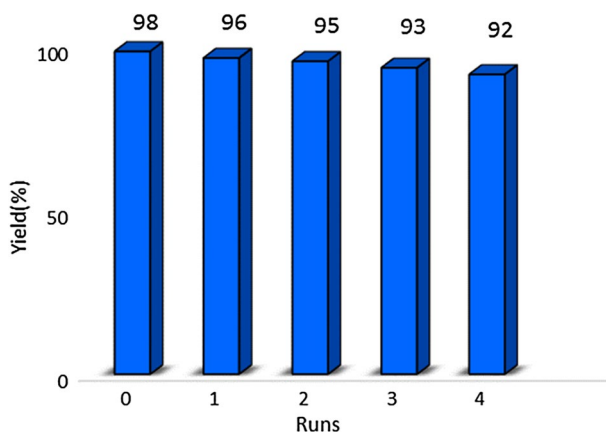
Fig. 6 Reusability of the ompg-C$_3$N$_4$/SO$_3$H catalyst in the model reaction

Fresh ompg-C3N4SO3H ——— Used ompg-C3N4/SO3H
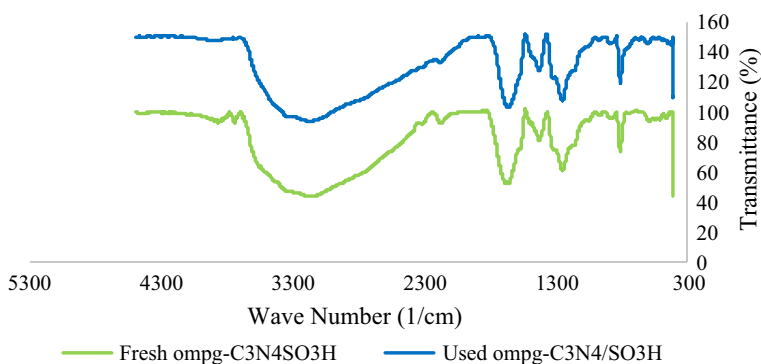
Fig. 7 FT-IR spectra of fresh and used ompg-C$_3$N$_4$/SO$_3$H

of (**II**) followed by a ring closure forming intermediate (**IV**) which undergoes intramolecular cyclization to afford target product (**3**).

One of the most important aspects of a heterogeneous catalyst in green chemistry is its stability and reusability. Hence, we evaluated the reusability of the ompg-C$_3$N$_4$/SO$_3$H for the synthesis of 2,3-dihydroquinazolin-4(1H)-ones. As the reaction went to completion, the catalyst was separated from the reaction mixture, washed with ethanol, and dried at 60 °C, then reused for the fresh reactions. It was found that the ompg-C$_3$N$_4$/SO$_3$H shows negligible loss in the catalytic activity after five cycles (Fig. 6).

The acidity of the catalyst after the reaction was determined through the back-titration method. The pH value of the used ompg-C$_3$N$_4$/SO$_3$H was calculated (pH = 1.55) as the same pH value as the fresh ompg-C$_3$N$_4$/SO$_3$H. These results indicate that the acidity of the ompg-C$_3$N$_4$/SO$_3$H did not change after the reaction. For further confirmation, FT-IR spectra of the fresh and used catalyst (ompg-C$_3$N$_4$/SO$_3$H)

Table 4 Comparison of the catalytic efficiency of ompg-C_3N_4/SO_3H with the previously reported catalysts for the synthesis of 2,3-dihydroquinazolin-4(1H)-one derivatives

Entry	Catalyst (amount of catalyst)	Solvent	Temp. (°C)	Time	Yield (%)	Ref.
1	$H_3PW_{12}O_{40}$ (1 mol%)	H_2O/CTAB	80	60 min	83	[44]
2	$Y(NO_3)_3.6H_2O$ (10 mol%)	CH_3CN	RT	5 h	98	[45]
3	SiO_2-$FeCl_3$ (5 mg)	–	80	6 h	87	[46]
4	$ZnFe_2O_4$ (30 mol%)	H_2O	MW	80 min	90	[47]
5	Boehmite-Si-DSA (30 mg)	EtOH	80	60 min	96	[48]
6	Ompg-C_3N_4/SO_3H (20 mg)	EtOH	80	3 min	98	This work

RT room temperature

was examined. As shown in Fig. 7, the ompg-C_3N_4/SO_3H had no obvious change after five cycles.

ompg-C_3N_4/SO_3H as an efficient and environmentally friendly organocatalyst for the synthesis of 2,3-dihydroquinazolin-4(1H)-one derivatives has some advantages in comparison with the other catalysts in the literature containing shorter reaction time and high yield (Table 4).

Conclusion

In conclusion, we have illustrated that ompg-C_3N_4/SO_3H can be utilized as an effective and eco-friendly organocatalyst for the one-pot synthesis of 2,3-dihydroquinazolin-4(1H)-one derivatives via the condensation of anthranilamide with carbonyl compounds (aldehydes and ketones) under mild conditions. The remarkable advantages of this novel protocol are mild reaction condition, short reaction times, simple work-up procedure, good to excellent yield of the products, and reusability of the catalyst without loss of activity.

References

1. G.M. Ziarani, A. Badiei, Z. Aslani, N. Lashgari, Arab. J. Chem. **8**, 54 (2015)
2. P. Gupta, S. Paul, Catal. Today **236**, 153 (2014)
3. J. Xu, G. Wang, J. Fan, B. Liu, S. Cao, J. Yu, J. Power Sources **274**, 77 (2015)
4. S. Yan, Z. Li, Z. Zou, Langmuir **25**, 10397 (2009)
5. X.L. Zhang, C. Zheng, S.S. Guo, J. Li, H.H. Yang, G. Chen, Anal. Chem. **86**, 3426 (2014)
6. Y.P. Yuan, S.W. Cao, Y.S. Liao, L.S. Yin, C. Xue, Appl. Catal. B **140**, 164 (2013)
7. X. Chen, J. Zhang, X. Fu, M. Antonietti, X. Wang, J. Am. Chem. Soc. **131**, 11658 (2009)
8. K.S. Lakhi, D.H. Park, K. Al-Bahily, W. Cha, B. Viswanathan, J.H. Choy, A. Vinu, Chem. Soc. Rev. **46**, 2 (2017)
9. J. Zhu, P. Xiao, H. Li, S.A. Carabineiro, ACS Appl. Mater. Interfaces **6**, 16449 (2014)
10. Z. Yang, Y. Zhang, Z. Schnepp, J. Mater. Chem. A **3**, 14081 (2015)
11. H. Li, L. Wang, Y. Liu, J. Lei, J. Zhang, Res. Chem. Intermed. **42**, 3979 (2016)

12. A. Sayari, Y. Yang, Chem. Mater. **17**, 6108 (2005)
13. H. Ghafuri, M. Talebi, Ind. Eng. Chem. Res. **55**, 2970 (2016)
14. A. Emami, H. Ghafuri, M.K. Kenari, A. Maleki, ChemistrySelect **3**, 6349 (2018)
15. H.R.E. Zand, H. Ghafuri, N. Ghanbari, ChemistrySelect **3**, 8229 (2018)
16. H. Ghafuri, A. Rashidizadeh, H.R.E. Zand, RSC Adv. **6**, 16046 (2016)
17. M.A.D. Fard, H. Ghafuri, A. Rashidizadeh, Microporous Mesoporous Mater. **274**, 83 (2019)
18. P. Sivaguru, K. Parameswaran, A. Lalitha, Mol. Divers. **21**, 611 (2017)
19. P. Salehi, M. Ayyari, M. Bararjanian, S.N. Ebrahimi, A. Aliahmadi, J. Iran. Chem. Soc. **11**, 607 (2014)
20. O.I. El-Sabbagh, S.M. Ibrahim, M.M. Baraka, H. Kothayer, Archiv der Pharmazie: int. J. Pharm. Med. Chem. **343**, 274 (2010)
21. S. Zhaleh, N. Hazeri, M.T. Maghsoodlou, Res. Chem. Intermed. **42**, 6381 (2016)
22. A. Davoodnia, S. Allameh, A. Fakhari, N. Tavakoli-Hoseini, Chin. Chem. Lett. **21**, 550 (2010)
23. M. Ghashang, S.S. Mansoor, K. Aswin, Res. Chem. Intermed. **41**, 3447 (2015)
24. S.U. Deshmukh, K.R. Kharat, G.G. Kadam, R.P. Pawar, Eur. J. Chem. **8**, 317 (2017)
25. M. Prakash, V. Kesavan, Org. Lett. **14**, 1896 (2012)
26. S.P. Bahekar, N.D. Dahake, P.B. Sarode, H.S. Chandak, Synlett **26**, 2575 (2015)
27. Y.S. Jun, W.H. Hong, M. Antonietti, A. Thomas, Adv. Mater. **21**, 4270 (2009)
28. Z. Zhao, Y. Dai, J. Lin, G. Wang, Chem. Mater. **26**, 3151 (2014)
29. J. Liu, J. Yan, H. Ji, Y. Xu, L. Huang, Y. Li, Y. Song, Q. Zhang, H. Xu, H. Li, Mater. Sci. Semicond. Process. **46**, 59 (2016)
30. J. Zhang, F. Guo, X. Wang, Adv. Funct. Mater. **23**, 3008 (2013)
31. A. Ghorbani-Choghamarani, P. Zamani, J. Iran. Chem. Soc. **9**, 607 (2012)
32. M. Singh, N. Raghav, Bioorg. Chem. **59**, 12 (2015)
33. M. Abdollahi-Alibeik, E. Shabani, J. Iran. Chem. Soc. **11**, 351 (2014)
34. R. Mekala, M. Madhubabu, G. Dhanunjaya, S. Regati, K. Chandrasekhar, J. Sarva, Synth. Commun. **47**, 121 (2017)
35. A. Maleki, M. Rabbani, S. Shahrokh, Appl. Organomet. Chem. **29**, 809 (2015)
36. M. Hajjami, F. Bakhti, E. Ghiasbeygi, Croat. Chem. Acta **88**, 197 (2015)
37. H.R. Safaei, M. Shekouhy, V. Shafiee, M. Davoodi, J. Mol. Liq. **180**, 139 (2013)
38. R. Ramesh, N. Nagasundaram, D. Meignanasundar, P. Vadivel, A. Lalitha, Res. Chem. Intermed. **43**, 1767 (2017)
39. S. Rostamizadeh, A.M. Amani, R. Aryan, H.R. Ghaieni, N. Shadjou. Synth. Commun. **38**, 3567 (2008)
40. A. Ghorbani-Choghamarani, B. Tahmasbi, New J. Chem. **40**, 1205 (2016)
41. F. Tamaddon, M. KazemiVarnamkhasti, Synlett **27**, 2510 (2016)
42. A.D. Gupta, S. Samanta, A.K. Mallik, Org. Prep. Proced. Int. **47**, 356 (2015)
43. S. Das, S. Santra, S. Jana, G.V. Zyryanov, A. Majee, A. Hajra, Europ. J. Org. Chem. **2017**, 4955 (2017)
44. M. Tajbakhsh, R. Hosseinzadeh, P. Rezaee, M. Tajbakhsh, Chin. J. Catal. **35**, 58 (2014)
45. A.A. Khan, K. Mitra, A. Mandal, N. Baildya, M.A. Mondal, Heteroat. Chem. **28**, 21379 (2017)
46. G. Majid, A. Kobra, M.P. Hamed, S.H. Reza, Chin. J. Chem. **29**, 1617 (2011)
47. B.D. Rupnar, T.R. Kachave, P.D. Jawale, S.U. Shisodia, R.P. Pawar, J. Iran. Chem. Soc. **14**, 1853 (2017)
48. M. Hajjami, A. Ghorbani-Choghamarani, R. Ghafouri-Nejad, B. Tahmasbi, New J. Chem. **40**, 3066 (2016)